

OPTICAL FIBRES

PACS numbers: 42.55.Wd; 42.81.Dp
DOI: 10.1070/QE2011v041n12ABEH014746

Luminescence and photoinduced absorption in ytterbium-doped optical fibres

A.A. Rybaltovsky, S.S. Aleshkina, M.E. Likhachev, M.M. Bubnov, A.A. Umnikov, M.V. Yashkov, A.N. Gur'yanov, E.M. Dianov

Abstract. **Photochemical reactions induced in the glass network of an ytterbium-doped fibre core by IR laser pumping and UV irradiation have been investigated by analysing absorption and luminescence spectra. We have performed comparative studies of the photoinduced absorption and luminescence spectra of fibre preforms differing in core glass composition: Al_2O_3:SiO_2, Al_2O_3:Yb_2O_3:SiO_2, and P_2O_5:Yb_2O_3:SiO_2. The UV absorption spectra of unirradiated preform core samples show strong bands peaking at 5.1 and 6.5 eV, whose excitation plays a key role in photoinduced colour centre generation in the glass network. 'Direct' UV excitation of the 5.1- and 6.5-eV absorption bands at 244 and 193 nm leads to the reduction of some of the Yb^{3+} ions to Yb^{2+}. The photodarkening of ytterbium-doped fibres by IR pumping is shown to result from oxygen hole centre generation. A phenomenological model is proposed for the IR-pumping-induced photodarkening of ytterbium-doped fibres. The model predicts that colour centre generation in the core glass network and the associated absorption in the visible range result from a cooperative effect involving simultaneous excitation of a cluster composed of several closely spaced Yb^{3+} ions.**

Keywords: *ytterbium-doped optical fibre, photodarkening, photochemical reactions, cooperative luminescence, oxygen hole centres.*

1. Introduction

The IR-pumping-induced increase in optical loss (photodarkening) in ytterbium-doped active optical fibres plays a critical role in limiting the service life of ytterbium fibre lasers and amplifiers. The photodarkening effect was first found in fibres doped with thulium [1] and terbium [2], and the first study of photodarkening in ytterbium-doped fibres was reported in 2005 by Koponen et al. [3], who showed that the photodarkening in the spectral range of ytterbium pumping and luminescence (900–1100 nm) was mainly due to the influence of the long-wavelength edge of the photoinduced absorption, with a peak below 600 nm. In 2007, Morasse et al. [4] showed that the long-wavelength absorption edge belonged to a broad band centred near 450 nm and that the photoinduced absorption spectra of fibres after IR pumping and UV exposure were essentially identical in shape. In nearly the same years, Koponen et al. [5–7] showed for the first time that the rate and maximum magnitude of photodarkening in IR-pumped ytterbium-doped fibre depended on the Yb^{3+} excited state population (inversion level). Analysis of the photoinduced absorption as a function of time and pump intensity led Koponen et al. [5–7] to assume that interaction between six to eight (on average, seven) excited Yb^{3+} ions was needed to produce one network defect responsible for the absorption in the visible range.

In 2006–2007, at least two more groups focused on the kinetics of IR-pumping-induced absorption in ytterbium-doped fibres. In 2007, Jetschke et al. [8] and Shubin et al. [9] reported their findings on photodarkening kinetics in fibre cores differing in ytterbium concentration. Following Koponen et al. [5–7], they relied on the assumption that cooperative interaction of excited Yb^{3+} ions played a key role in initiating the photochemical reactions behind the formation of network defects responsible for the absorption in the visible range. There are, however, widely different estimates for the number of interacting ions needed for defect generation. According to Shubin et al. [9], the photodarkening rate varies as the fifth power of the excited Yb^{3+} concentration, and five, rather than seven [5–7], ions should interact to produce one network defect. At the same time, according to Jetschke et al. [8] the mean number of simultaneously interacting ions is even smaller: just three or four ions per defect. Note, however, that neither the mechanism of the interaction nor the nature of the defects involved has been discussed in detail in Refs [5–9].

Nevertheless, the first attempts to interpret photodarkening in ytterbium-doped fibres in terms of particular photochemical reactions and colour centres in the core glass were made at nearly the same time when this effect attracted increased interest: in 2006–2007. In those years, research emerged that focused on analysis of the photodarkening mechanism in terms of glass network elements and defects. In particular, Jasapara et al. [10] and Engholm and Norin [11] were the first to hypothesise that the effect was due to photochemical reactions involving not only trivalent but also divalent ytterbium (Yb^{2+}). There is another, no less widespread, opinion [12–14], that a key role is played not by Yb^{2+} ions but by oxygen-deficient centres (ODCs). Thus, there are currently at least two radically different approaches to interpreting the photodarkening effect. Unfortunately, both are incapable of accounting for all experimental data available in the literature.

A.A. Rybaltovsky, S.S. Aleshkina, M.E. Likhachev, M.M. Bubnov, E.M. Dianov Fiber Optics Research Center, Russian Academy of Sciences, ul. Vavilova 38, 119333 Moscow, Russia;
e-mail: andy@fo.gpi.ru, sv-alesh@yandex.ru, likhachev@fo.gpi.ru, bubnov@fo.gpi.ru, dianov@fo.gpi.ru;
A.A. Umnikov, M.V. Yashkov, A.N. Gur'yanov Institute of Chemistry of High-Purity Substances, Russian Academy of Sciences, ul. Tropinina 49, 603950 Nizhnii Novgorod, Russia;
e-mail: umnikov@ihps.nnov.ru, yashkovmv@yandex.ru, tvs@ihps.nnov.ru

Received 5 November 2011
Kvantovaya Elektronika **41** (12) 1073–1079 (2011)
Translated by O.M. Tsarev

Table 1. Main characteristics of the samples.

Sample	Al_2O_3 content (mol %)	P_2O_5 content (mol %)	Yb content (wt %)	Core–cladding index difference
A0	1.8	0	0	0.0045
A1	2.3	0	1.5	0.007
P1	0	6.5	1.1	0.006

Starting in 2008, intensive research effort has been concentrated on approaches that would allow the photodarkening loss to be completely eliminated or at least minimised. It has been shown that the photoinduced absorption can be reduced severalfold or even by an order of magnitude in fibres having a multicomponent core [15, 16] or loaded with molecular hydrogen [17] and also by heating the fibre to ~600 K [17–19]. Detailed analysis of such results provided considerable insight into the defect structure. In particular, the photoinduced absorption in the visible range was identified as due to ODCs [17]. Nevertheless, the mechanism of the visible–IR absorption induced in ytterbium-doped fibres by prolonged IR pumping and that of its relaxation are still poorly understood.

In this paper, we propose a model, common to ytterbium-doped alumino- and phosphosilicate fibres, for colour centre generation in core glass by IR pumping (920–980 nm) or UV exposure (below 250 nm). The model was derived by analysing reported and experimentally determined initial and photoinduced absorption and photoluminescence spectra of ytterbium-doped fibres and preforms differing in core glass composition.

2. Experimental

Fibre preforms were produced by MCVD and were then drawn into multimode fibres 125 μm in outer diameter. The preforms and fibres were divided into three groups, depending on the core glass composition: A0, aluminosilicate glass ($Al_2O_3:SiO_2$); A1, ytterbium-doped aluminosilicate glass ($Al_2O_3:Yb_2O_3:SiO_2$); and P1, ytterbium-doped phosphosilicate glass ($P_2O_5:Yb_2O_3:SiO_2$). The chemical composition of the preforms was determined with an accuracy of 0.1 wt % on a JEOL JSM-5910LV equipped with an X-ray microanalysis system. It is important to note that, in contrast to previous studies, we did not use $GeCl_4$ in any of the preform fabrication steps, so the presence of GeO_2 in the core glass network in our samples can be completely ruled out. The refractive index profiles across the preforms were obtained with a York Technology P102 preform analyser. The refractive indices of the core and cladding were determined with an accuracy of 0.0005. The chemical compositions and index contrasts of the preforms are given in Table 1.

Initial and photoinduced absorption spectra in the UV and visible spectral regions (190–800 nm) and luminescence spectra were taken using 0.2-, 0.5- and 1-mm-thick transverse sections of the preforms. In addition, we measured visible absorption spectra of 5- to- 50-cm-long fibres. The absorption spectra of the preforms were obtained on a PerkinElmer Lambda 900 spectrophotometer, and those of the fibres were taken with a measuring system built around an MDR-6 monochromator (LOMO PLC). Luminescence spectra were measured on an Ocean Optics QE65000 minispectrometer in the range 200–1000 nm and on a Hewlett-Packard Model 70950B optical spectrum analyser in the range 900–1100 nm.

The preforms were irradiated by focusing a laser beam onto the core area, and the fibres, by launching a beam into their core. The irradiation conditions are summarised in Table 2. Note that the transverse sections of the preforms were irradiated in the UV spectral region (lasers L1 and L2), and the fibres, in the visible and IR (lasers L3 and L4). Since the pump diode laser L4 had an output fibre pigtail, its beam was coupled into the fibre core through a fusion splice. During irradiation, the luminescence of the preform or fibre was detected at 90° to the beam direction using a multimode silica glass (KU-1) core fibre coupled to a spectrometer (spectrum analyser).

All irradiations, as well as the luminescence and photoinduced absorption measurements, were performed at room temperature (~300 K).

3. Results and discussion

Figure 1 presents the absorption spectra of the Yb_2O_3-doped preforms (A1 and P1) before irradiation. Note that the absorption in samples A0 in the spectral range represented in Fig. 1 was negligible (within 0.1 cm^{-1}). Therefore, ytterbium doping of the core glass increases the absorption in the UV spectral region by more than two orders of magnitude. Moreover, the transmission spectrum of preforms A1 shows a prominent absorption band peaking at ~5 eV (240 nm), whereas the spectrum of samples P1 contains no such band. Analysis of the absorption spectrum by standard fitting with Gaussians [20] showed that the optical loss spectrum of samples A1 in the range 180–400 nm consisted mainly of two absorption bands, peaking at 5.1 and 6.5 eV. Using the same fitting procedure for modelling the absorption spectrum of samples P1, we identified an absorption band peaking at 6.7 eV.

There are currently several hypotheses as to the origin of the 5-eV band in the absorption spectra of $Al_2O_3:Yb_2O_3:SiO_2$ preforms. For example, Yoo et al. [12] assigned this band to ytterbium-related ODCs (Yb–Yb centres), which were assumed to be present in the glass network by analogy

Table 2. Preform and fibre irradiation conditions.

Source	Wavelength/nm	Photon energy/eV	Intensity/W cm^{-2}	Fluence/J cm^{-2}
CL-5000 ArF laser (L1)	193	6.4	10^7	3×10^2
Spectra Physics 2040E				
Ar^+ laser (L2)	244	5.1	10	10^5
Spectra Physics 165				
Kr^+ laser (L3)	476	2.6	3×10^3	10^8
EM4 diode laser (L4)	920	1.35	4×10^4	2×10^8

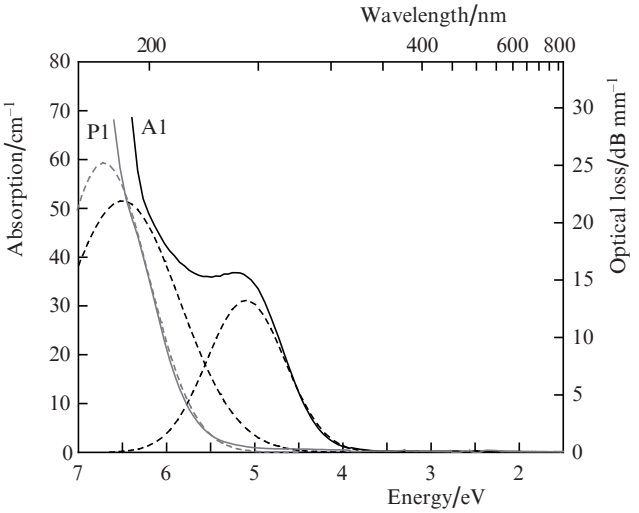

Figure 1. Initial transmission spectra of samples A1 and P1 in the UV and visible spectral regions. The solid lines represent experimental data and the dashed lines represent the Gaussian components of the spectra.

with the structure and properties of germanium-related ODCs in the germanosilicate glass network. Such centres can be described in terms of the neutral oxygen vacancy model [21]. The 5-eV band was also attributed to ODCs by Dragic et al. [13] and Carlson et al. [14], but they thought the ODCs to be related not to ytterbium but to germanium or silicon [22].

There are, however, other interpretations of the UV absorption spectrum of ytterbium-doped silica glass. For example, in their studies of photodarkening in ytterbium-doped fibres, Engholm et al. [23–26] criticised the hypothesis that the 5-eV band was due to ODCs and assigned the UV absorption in the range 180–400 nm to di- and trivalent ytterbium ions (Yb^{2+} and Yb^{3+}). In particular, the absorption near 240 nm was thought to be contributed primarily by two bands: an Yb^{3+} charge transfer (CT) band and a band due to the transition of the Yb^{2+} ion from the $4f^{14}$ to the $4f^{13}5d$ state. This assumption was based mainly on comparison of the observed absorption and luminescence spectra of the fibres with the spectra of ytterbium-doped crystals [27, 28].

It should be noted that the UV absorption spectrum of Yb^{2+} in silica glass shows not only the 240-nm band but also three other, weaker bands: 400 (3.1 eV), 330 (3.8 eV) and 300 nm (4.1 eV) [29, 30]. It follows from analysis of the spectra reported by Kovaleva et al. [29] and Kirchhof et al. [30] for silica glass whose network initially contained some of the ytterbium ions in the form of Yb^{2+} that the 400-nm band was more than one order of magnitude weaker than the 240-nm band and that the 330- and 300-nm bands were, respectively, about a factor of 7 and 3 weaker than the 240-nm band. At the same time, the absorption spectrum of sample A1 (Fig. 1) has only one band, peaking at 240 nm, and there is nearly zero absorption at wavelengths above 350 nm. Thus, it seems likely that, before irradiation, the glass network in our samples contained no Yb^{2+}, and all the ytterbium was present in the form of Yb^{3+}.

In contrast, irradiation (especially that with high-energy, UV photons) produced spectral changes that suggested that some of the Yb^{3+} ions converted to a divalent state. In particular, the luminescence spectra of samples A1 and P1 contained a strong band centred at 550 nm [Fig. 2, spectra (*1*–*4*)], attributable to a transition of Yb^{2+} from the charge transfer state to a $4f^{14}$ state [31]. Moreover, the 550-nm (2.3-eV) band in the spectra of our samples may be due to Yb^{3+} radiative relaxation from the charge transfer state to the $^2F_{5/2}$ level, corresponding to a lower energy excited state [32, 33]. According to the assignment by Guerassimova et al. [32] and Krasikov et al. [33], the bands at 3.6 and 3.2 eV in the luminescence spectra of samples A1 and P1 are then also due to Yb^{3+} radiative relaxation from the charge transfer state, but to the $^2F_{7/2}$ ground level. They pointed out that some of the UV-excited Yb^{3+} ions formed centres with Yb^{2+} instead of relaxing to their initial state. According to Nizamutdinov et al. [34] and Kazcmarek et al. [35], the conversion of some of the excited Yb^{3+} ions to Yb^{2+} is caused by the capture of conduction band electrons.

The $Yb^{3+} \rightarrow Yb^{2+}$ conversion process seems to be contributed by the UV ionisation of ODCs near ytterbium atoms, as evidenced by the strong luminescence bands at wavelengths under 400 nm (Fig. 2). These bands are particularly prominent in the luminescence spectrum of undoped SiO_2 [Fig. 2, spectrum (*6*)]. Fitting this spectrum with Gaussians (Fig. 2, inset) demonstrates that it consists of two components, centred at 4.1 and 3.2 eV. The 4.1-eV band corresponds to the luminescence of well-known silicon-related ODCs [22], and the 3.2-eV band is due to ODCs 'modified' by neighbouring aluminium, phosphorus or fluorine atoms [36].

It seems likely that most of the UV-excited Yb^{3+} ions merely relax to the ground state and that the relaxation process is accompanied by IR luminescence (Fig. 3). Its spectrum is very similar to the emission spectrum of ytterbium-doped fibres under excitation in the range 920–980 nm [37, 38]. Figure 3 shows only IR luminescence spectra under excitation by laser L1 (193 nm) because the spectra of samples A1 and P1 under excitation at 244 nm (laser L2) were identical in shape to spectra (*1*) and (*2*) in Fig. 3.

When samples A1 and P1 were irradiated with laser L4 (920 nm), we observed, in addition to strong Yb^{3+} IR luminescence, a 'green' luminescence centred around 500 nm. This

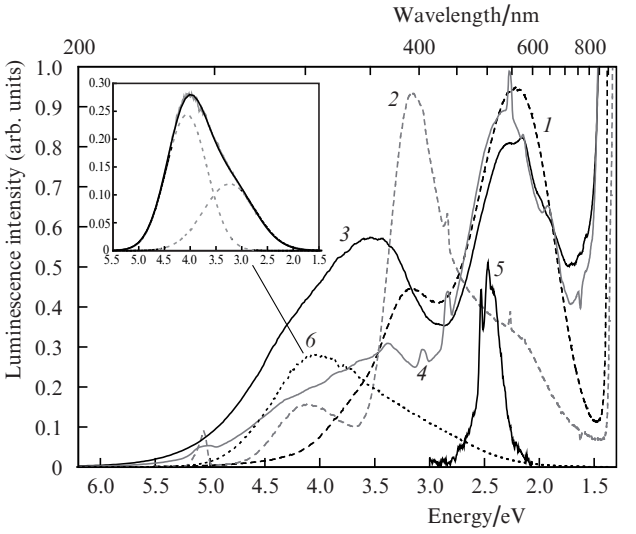

Figure 2. UV to visible luminescence spectra under excitation with different sources: (*1*) sample P1, excitation with laser L1; (*2*) P1, L2; (*3*) A1, L1; (*4*) A1, L2; (*5*) A1, L4; (*6*) undoped preform (pure SiO_2), L1. Inset: decomposition of spectrum (*6*) into Gaussian components.

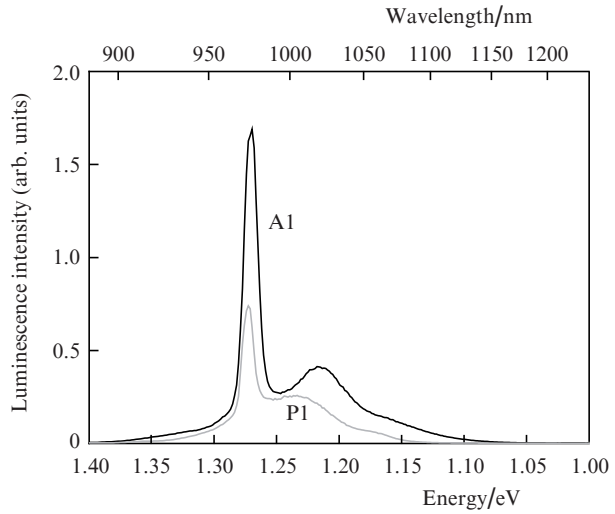

Figure 3. IR luminescence spectra of samples A1 and P1 under excitation with laser L1.

luminescence is known as cooperative ytterbium luminescence [39] because it is commonly assigned to the interaction between two Yb^{3+} ions ('ion pairs') [40–42]. According to Guzman-Chavez et al. [43], this interaction can initiate partial Yb^{3+} conversion to Yb^{2+}, like in the case of UV exposure. Analysis of the spectra in Fig. 2 shows however that the reduction of Yb^{3+} to Yb^{2+} under UV irradiation is accompanied by the ionisation of ODCs, which act as an extra source of conduction band electrons. Under 920-nm irradiation, UV luminescence, indicative of processes related to ODC ionisation, was not detected. Thus, the $Yb^{3+} \rightarrow Yb^{2+}$ conversion intensity under IR excitation seems to be far lower than that under UV irradiation. Moreover, it is seen in Fig. 2 that the Yb^{3+}–Yb^{3+} cooperative luminescence peak position [spectrum (*5*)] essentially coincides with the peak position of the luminescence related to Yb^{2+} or Yb^{3+} radiative relaxation from the charge transfer state [spectra (*1–3*)]. Therefore, the weak charge transfer luminescence signal is difficult to detect in the presence of strong ion-pair luminescence under IR excitation (and conversely, the cooperative luminescence signal is difficult to detect in the presence of strong charge transfer luminescence under UV excitation).

Nevertheless, we tried to detect luminescence related to the $Yb^{3+} \rightarrow Yb^{2+}$ conversion process not via excitation of the Yb^{3+} IR absorption band but via 'direct' excitation of Yb^{3+}– Yb^{3+} ion pairs by a visible light source with a wavelength close to that of the absorption band of ion pairs (472 nm) found by Kir'yanov et al. [42]. Note that a similar experiment had been carried out previously [42–44]. According to Kir'yanov et al. [44], the spectrum of samples exposed to an Ar^+ laser beam (488 nm) shows both visible (centred at $\lambda \sim 480$ nm) and IR luminescence bands, due to ion pairs and single Yb^{3+} ions. Moreover, in the spectral range 600–900 nm, Kir'yanov et al. [44] detected a broad (~200 nm), weak luminescence band, which was tentatively attributed to the Yb^{2+} ions resulting from the $Yb^{3+} \rightarrow Yb^{2+}$ conversion process.

Using the experimental procedure described by Kir'yanov et al. [44] and laser L3 (476 nm), we attempted to reveal luminescence related to the excitation of ion pairs in our samples. However, neither visible not IR luminescence characteristic of Yb^{3+} was detected, even though the efficiency of the action of photons with $\lambda = 476$ nm (very close to the peak absorption wavelength) on ion pairs should markedly exceed that of 488-nm radiation, used by Kir'yanov et al. [44]. Thus, the luminescence spectrum we observed differs qualitatively from the spectra reported in Ref. [44], and this can be accounted for by either the considerably higher (by more than one order of magnitude) concentration of Yb^{3+}–Yb^{3+} ion pairs in the core glass in Ref. [44] or the presence of other rare-earth ions, e.g. Tm^{3+}, capable of sharply raising the photosensitivity in the visible range [45, 46].

In addition to the luminescence spectra, we examined photoinduced absorption spectra of samples irradiated at the same wavelengths as were used to excite their luminescence. Figure 4 shows the absorption spectra of samples A0, A1 and P1 after irradiation at 920 [spectrum (*1*)], 244 [spectrum (*2*)] and 193 nm [spectra (*3–5*)]. Irradiation at 476 nm produced no changes in the absorption spectra of our samples. Nor were any significant changes detected in the absorption spectrum of sample A0 or P1 after irradiation at 920 or 244 nm. The lack of photoinduced absorption in samples A0 after irradiation at 244, 476, and 920 nm is mainly due to the high transmission of undoped aluminosilicate glass at wavelengths above 200 nm. By contrast, irradiation of samples A0 at $\lambda =$ 193 nm gives rise to absorption bands due to photoinduced defects (colour centres) in the glass network. In particular, analysis of the shape of spectrum (*4*) in Fig. 4 and comparison with published data for colour centres in aluminosilicate glass [47, 48] allowed us to identify five photoinduced absorption bands, centred at 2.3, 3.2, 4.1, 5.5 and 5.7 eV.

The 2.3- and 3.2-eV bands correspond to aluminium–oxygen hole centres (Al-OHCs), the 4.1-eV band is due to the aluminium electron centre (AlE′), and the closely spaced bands at 5.5 and 5.7 eV arise from two types of silicon electron centres (SiE'_2 and SiE′). These colour centres and the corresponding absorption bands seem to emerge upon irradiation of samples A1, which differ from samples A0 in that their glass network contains ytterbium ions. For example, analysis of the shape of spectra (*1–4*) in Fig. 4 from 400 to 700 nm demonstrates that Al-OHCs and the associated absorption result from both UV and IR irradiations. At the

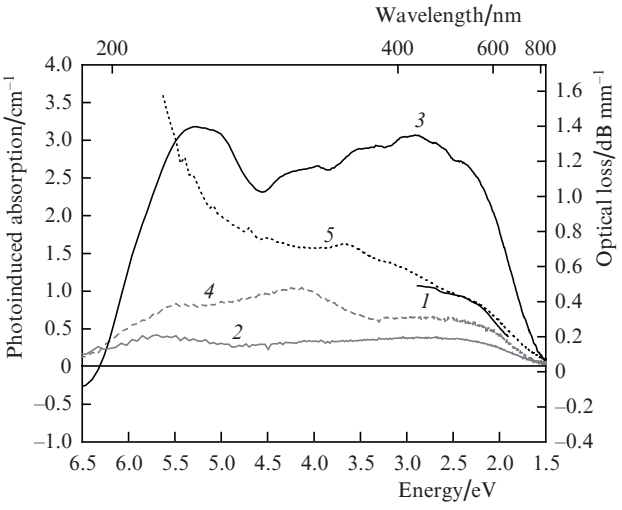

Figure 4. Photoinduced absorption spectra after irradiation of the samples with different light sources: (*1*) sample A1 (fibre), irradiation with laser L4; (*2*) A1, L2; (*3*) A1, L1; (*4*) A0, L1; (*5*) P1, L1.

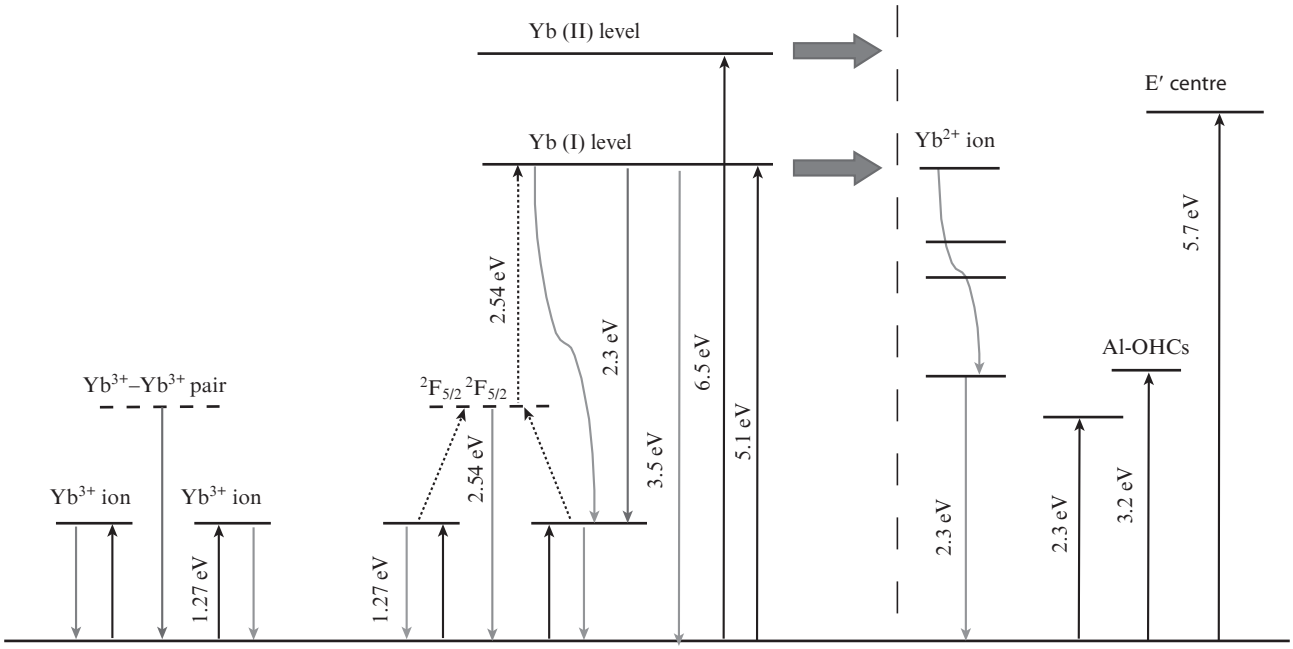

Figure 5. Model of colour centre generation in the $Al_2O_3:Yb_2O_3:SiO_2$ glass network by IR pumping and UV irradiation.

same time, there are a number of distinctions between the photoinduced absorption spectra of samples A0 and A1. In particular, the spectrum of sample A1 after irradiation at λ = 193 nm [Fig. 4, spectrum (*3*)] shows a strong band peaking at ~5.2 eV, in contrast to the spectrum of sample A0 after irradiation under the same conditions. Analysis of the present luminescence spectra and the hypotheses set forth by Engholm et al. [23] and Kazcmarek et al. [35] lead us to assume that this band is due to the Yb^{2+} ions resulting from the $Yb^{3+}\rightarrow Yb^{2+}$ conversion by high-energy (6.4 eV) UV photons.

It is of interest to compare the photoinduced absorption spectra of samples A1 and P1 after irradiation at 193 nm [Fig. 4, spectra (*3*, *5*)]. According to Hosono et al. [49], 193-nm irradiation of phosphosilicate glass produces phosphorus–oxygen hole centres (P-OHCs), which have two absorption bands in the visible range, centred at 2.2 and 3.2 eV. It seems likely that such centres are also produced by UV irradiation in the glass network of samples P1 and that the similar optical properties of the aluminium–oxygen and phosphorus–oxygen hole centres are responsible for the similarity between the photoinduced absorption spectra of samples A0, A1 and P1 in the range 400–800 nm. Moreover, we assume that P-OHCs and their absorption bands may also result from IR irradiation and that this absorption underlies the photodarkening of ytterbium-doped phosphosilicate fibres studied previously [9, 17]. Note, however, that the absorption induced in $P_2O_5:Yb_2O_3:SiO_2$ fibres by IR irradiation is an order of magnitude weaker than that in $Al_2O_3:Yb_2O_3:SiO_2$ fibres, which can be accounted for under the assumption that the 5.1-eV absorption band, missing in the spectra of samples P1, is mainly due to the oxygen hole centres produced in the glass network by IR irradiation.

We propose here a phenomenological model of colour centre generation in the glass network of an ytterbium-doped fibre core by IR or UV irradiation. In Fig. 5, the model is represented as a diagram of possible photochemical reactions in $Al_2O_3:Yb_2O_3:SiO_2$ glass. We assume that the $Yb^{3+}–Yb^{3+}$ ion pairs include centres responsible for the absorption bands at 5.1 and 6.7 eV [the corresponding transitions in Fig. 5 are designated as transitions to the Yb(I) and Yb(II) levels]. Ishii [50] presented theoretical calculation results for the ground and excited states of a close analogue of ion pairs in the glass network: an $Yb^{3+}–O–Yb^{3+}$ dimer in $Y_3Al_5O_{12}$ and Y_2O_3 crystals. According to his calculations, this complex in an excited state has absorption lines at 20 000 cm^{-1} (2.5 eV). Based on his numerical modelling results, we assume that excited ion pairs in the $Al_2O_3:Yb_2O_3:SiO_2$ glass network also produce a system of levels near 2.5 eV. Thus, according to this hypothesis and ion pair models described in Refs [42, 50], simultaneous excitation of two closely spaced ion pairs may lead to absorption of the net energy of one ion pair (2.54 eV) by the other pair. Since the net energy is then 5.08 eV, it is possible to excite a level of the centre responsible for the 5.1-eV band.

The addition of the energies of two ion pairs is equivalent to the action of a UV photon on the glass network, which may lead to rearrangement of the bonds between ytterbium atoms and their nearest neighbour environment, in particular to the formation of E′ electron centres, Al-OHC hole centres, and Yb^{2+}. It seems likely that three simultaneously excited ion pairs may interact in the same way, which would be sufficient to excite a 6.7-eV level, even though the probability of 'cooperative' interaction between three ion pairs (six closely spaced Yb^{3+} ions) should be considerably lower than that of interaction between two pairs (four Yb^{3+} ions) because, most likely, it depends significantly on both the initial ytterbium concentration in the glass network and the percentage of ions in an excited state (in other words, on the $^2F_{5/2}$ inverted population).

Since the absorption spectrum of samples P1 shows no band at 5.1 eV, photochemical reactions in the $P_2O_5:Yb_2O_3:SiO_2$ glass network can only be initiated by interaction between three (or more) closely spaced ion pairs. Then, when applying the scheme of photochemical reactions in Fig. 5 to the $P_2O_5:Yb_2O_3:SiO_2$ glass network, the Yb(I) level (5.1 eV) should be deleted, and all the changes in glass network repre-

sented in Fig. 5 (formation of Yb^{2+}, oxygen hole centres and E′ centres) will only be related to the excitation and relaxation of the Yb(II) level (6.7 eV).

4. Conclusions

We have studied the absorption spectra of preforms and fibres differing in core glass composition: $Al_2O_3:Yb_2O_3:SiO_2$ and $P_2O_5:Yb_2O_3:SiO_2$. The UV absorption spectra of unirradiated samples showed two main bands, peaking at 6.5 and 5.1 eV. The 5.1-eV absorption band was missing in the spectrum of the $P_2O_5:Yb_2O_3:SiO_2$ samples, whereas the 6.5-eV band was present in the spectra of samples with both compositions.

The luminescence spectra obtained under IR and UV excitation are analysed and compared. Under UV excitation, we observe a strong band centred at 2.3 eV, indicative of the reduction of some of the Yb^{3+} ions to a divalent state (Yb^{2+}). Most of the UV-excited Yb^{3+} ions relax, which is accompanied by IR luminescence with a peak emission wavelength of 975 nm (1.27 eV), characteristic of trivalent ytterbium.

Analysis of photoinduced absorption spectra indicates that the excitation of the 5.1- and 6.5-eV absorption bands by UV laser radiation at 244 and 193 nm leads to photoinduced absorption in the visible range, similar in shape to that under 920-nm irradiation. It has been identified as due to aluminium–oxygen or phosphorus–oxygen hole centres (Al-OHCs and P-OHCs), depending on glass composition.

The proposed phenomenological model for the IR-pumping-induced photodarkening of ytterbium-doped fibres predicts that colour centre generation in the glass network (Yb^{2+}, oxygen hole centres and E′ centres) and the associated absorption in the visible range result from a cooperative effect involving simultaneous excitation of several closely spaced Yb^{3+} ion pairs and subsequent excitation energy transfer to the transitions responsible for the absorption bands at 5.1 and 6.5 eV.

Acknowledgements. We are grateful to our colleagues at the Fiber Optics Research Center, Russian Academy of Sciences: to O.I. Medvedkov for his assistance in the experimental work and to V.G. Plotnichenko, A.V. Shubin and M.A. Mel'kumov for fruitful discussions and conversations.

References

1. Broer M.M., Krol D.M., Di Giovanni D.J. *Opt. Lett.*, **18** (10), 799 (1993).
2. Atkins G.R., Carter A.L.G. *Opt. Lett.*, **19** (12), 874 (1994).
3. Koponen J., Söderlund M.J., Tammela S.K.T., Po H. *Proc. SPIE–Int. Soc. Opt. Eng.*, **5990**, 599008 (2005).
4. Morasse B., Chatigny S., Gagnon E., Hovington C., Martin J.-P., de Sandro J.-P. *Proc. SPIE–Int. Soc. Opt. Eng.*, **6453**, 64530H (2007).
5. Koponen J., Söderlund M.J., Hoffman H.J., Tammela S.K.T. *Opt. Express*, **14** (24), 11539 (2006).
6. Koponen J., Söderlund M.J., Hoffman H.J., Kliner D.A.V., Koplow J.P., Hotoleanu M. *Appl. Opt.*, **47** (9), 1247 (2008).
7. Koponen J., Laurila M., Hotoleanu M. *Appl. Opt.*, **47** (25), 4522 (2008).
8. Jetschke S., Unger S., Röpke U., Kirchhof J. *Opt. Express*, **15** (22), 14838 (2007).
9. Shubin A., Yashkov M., Melkumov M., Smirnov S., Bufetov I., Dianov E. *Proc. Conf. CLEO/Europe-IQEC 2007* (Germany, Munich, CJ3-1-THU, 2007).
10. Jasapara J., Andrejco M., DiGiovanni D., Windeler R. *Proc. Conf. CLEO 2006* (Long Beach, California, USA, CTuQ5, 2006).
11. Engholm M., Norin L. *Proc. Photon. Appl., Systems & Technologies Conf. (PhAST-2007)* (Baltimore, Maryland, USA, JTuA61, 2007).
12. Yoo S., Basu C., Boyland A.J., Sones C., Nilsson J., Sahu J.K., Payne D. *Opt. Lett.*, **32** (12), 1626 (2007).
13. Dragic P.D., Carlson C.G., Croteau A. *Opt. Express*, **16** (7), 4688 (2008).
14. Carlson C.G., Keister K.E., Dragic P.D., Croteau A., Eden J.G. *J. Opt. Soc. Am. B*, **27** (10), 2087 (2010).
15. Jetschke S., Unger S., Schwuchow A., Kirchhof J. *Opt. Express*, **16** (20), 15540 (2008).
16. Engholm M., Jelger P., Laurell F., Norin L. *Opt. Lett.*, **34** (8), 1285 (2009).
17. Shubin A.V., Rybaltovsky A.A., Tomashuk A.L., Melkumov M.A., Yashkov M.V., Guryanov A.N., Bufetov I.A., Dianov E.M. *Proc. 18th Intern. Laser Phys. Workshop (LPHYS'09)* (Spain, Barcelona, 2009).
18. Leich M., Röpke U., Jetschke S., Unger S., Reichel V., Kirchhof J. *Opt. Express*, **17** (15), 12588 (2009).
19. Leich M., Jetschke S., Unger S., Kirchhof J. *Proc. SPIE–Int. Soc. Opt. Eng.*, **7580**, 758009 (2010).
20. Gusev E.V., Turoverov K.K. *J. Appl. Spectrosc.*, **29** (1), 844 (1978).
21. Sulimov V.B., Sokolov V.O., Dianov E.M., Poumellec B. *Kvantovaya Elektron.*, **23** (11), 1013 (1996) [*Quantum Electron.*, **26**, 988 (1996)].
22. Skuja L.J. *J. Non-Cryst. Solids*, **239**, 16 (1998).
23. Engholm M., Norin L., Aberg D. *Opt. Lett.*, **32** (22), 3352 (2007).
24. Engholm M., Norin L. *Proc. SPIE–Int. Soc. Opt. Eng.*, **6873**, 68731E (2008).
25. Engholm M., Norin L. *Opt. Express*, **16** (2), 1260 (2008).
26. Engholm M., Norin L. *Proc. SPIE–Int. Soc. Opt. Eng.*, **7195**, 71950T (2009).
27. Pieterson L., Heeroma M., Heer E., Meijerink A. *J. Lumin.*, **91**, 177 (2000).
28. Lizzo S., Klein Nagelwoort E.P., Erens R., Meijerink A., Blasse G. *J. Phys. Chem. Solids*, **58** (6), 963 (1997).
29. Kovaleva I.V., Kolobkov V.P., Starostina G.P. *Fiz. Khim. Stekla*, **12** (2), 222 (1986).
30. Kirchhof J., Unger S., Schwuchow A., Grimm S., Reichel V. *J. Non-Cryst. Solids*, **352**, 2399 (2006).
31. Reut E.G. *Opt. Spektrosk.*, **41** (1), 99 (1976).
32. Guerassimova N., Kamenskikh I., Krasikov D., Mikhailin V., Zagumennyi A., Koutovoi S., Zavartsev Yu., Pedrini C. *Radiat. Meas.*, **42**, 874 (2007).
33. Krasikov D.N., Scherbinin A.V., Vasil'ev A.N., Kamenskikh I.A., Mikhailin V.V. *J. Lumin.*, **128**, 1748 (2008).
34. Nizamutdinov A.S., Semashko V.V., Naumov A.K., Abdulsabirov R.Yu., Korableva S.L., Marisov M.A. *Fiz. Tverd. Tela*, **47** (8), 1403 (2005).
35. Kazcmarek S.M., Tsuboi T., Ito M., Boulon G., Leniec G. *J. Phys. Condens. Matter*, **17**, 3771 (2005).
36. Trukhin A.N., Golant K.M. J. *Non-Cryst. Solids*, **353**, 530 (2007).
37. Mel'kumov M.A., Bufetov I.A., Kravtsov K.S., Shubin A.V., Dianov E.M. *Kvantovaya Elektron.*, **34** (9), 843 (2004) [*Quantum Electron.*, **34** (9), 843 (2004)].
38. Kurkov A.S., Dianov E.M. *Kvantovaya Elektron.,* **34** (10), 881 (2004) [*Quantum Electron.*, **34** (10), 881 (2004)].
39. Magne S., Querdane Y., Druetta M., Goure J.P., Ferdinand P., Monnom G. *Opt. Commun.*, **111**, 310 (1994).
40. Chen Z., Freedhoff E. *Phys. Rev A*, **44** (1), 546 (1991).
41. Chen X., Li S., Song Z., Du W., Wen O., Sawanobori N. *J. Opt. Soc. Am. B*, **23** (12), 2581 (2006).
42. Kir'yanov A.V., Barmenkov Y.O., Martinez I.L., Kurkov A.S., Dianov E.M. *Opt. Express*, **14** (9), 3981 (2006).
43. Guzman-Chavez A.D., Kir'yanov A.V., Barmenkov Y.O., Il'ichev N.N. *Laser Phys. Lett.*, **4** (10), 734 (2007).
44. Kir'yanov A.V., Barmenkov Y.O., Mendoza-Santoyo F., Cruz J.L., Andres M.V. *Laser Phys. Lett.*, **5** (12), 898 (2008).
45. Peretti R., Jurdyc A-M., Jacquier B., Gonnet C., Pastouret A., Burov E., Cavani O. *Opt. Express*, **18** (19), 20455 (2010).
46. Jetschke S., Leich M., Unger S., Schwuchow A., Kirchhof J. *Opt. Express*, **19** (15), 14473 (2011).

47. Hosono H., Kawazoe H. *Nucl. Instrum. Methods Phys. Res., Sect. B*, **91** 395 (1994).
48. Trukhin A.N., Teteris J., Fedotov A., Griscom D.L., Buscarino G. *J. Non-Cryst. Solids*, **355**, 1066 (2009).
49. Hosono H., Kajihara K., Hirano M., Oto M. *J. Appl. Phys.*, **91** (7), 4121 (2002).
50. Ishii T. *J. Chem. Phys.*, **122**, 024705 (2005).